Chemical Engineering Science xxx (2017) xxx–xxx

Contents lists available at ScienceDirect

Chemical Engineering Science

journal homepage: www.elsevier.com/locate/ces

A mesoscale approach for population balance modeling of bubble size distribution in bubble column reactors

Ning Yang [a,*], Qi Xiao [a,b]

[a] State Key Laboratory of Multiphase Complex Systems, Institute of Process Engineering, Chinese Academy of Sciences, P.O. Box 353, Beijing 100190, PR China
[b] Wuhan 2nd Ship Design and Research Institute, Wuhan 430064, Hubei Province, PR China

HIGHLIGHTS

- We propose a new physical constraint to population balance equations.
- It is relevant to the mesoscale energy dissipation due to breakage and coalescence.
- A correction factor for coalescence rate is then derived from the new constraint.
- CFD-PBM simulation of bubble size with the new corrector agrees with experiments.
- The new corrector model can adapt the kernel functions used.

ARTICLE INFO

Article history:
Received 31 August 2016
Received in revised form 19 December 2016
Accepted 12 January 2017
Available online xxxx

Keywords:
Bubble size distribution
Population balance equation
Mesoscale
Coalescence
Breakage
Computational fluid dynamics

ABSTRACT

Prediction of bubble size distribution is of paramount importance for the study of bubble column reactors. Current kernel functions for coalescence or breakage in CFD-PBM simulation are usually derived from the isotropic turbulence theory and overestimate bubble size distribution with increasing gas flow rate. Based on the energy-minimization multi-scale concept, we develop a new approach to calculate the coalescence rate through the so-called stability condition and the meso-scale energy dissipation relevant to bubble breakage and coalescence (Yang et al., 2010). The approach is independent of specific kernel functions, and provides a new constraint to the kernel functions of coalescence or breakage which were previously only related to the turbulence properties through isotropic turbulence theory. New correctors for coalescence rate could then be derived for various kernel models. Our simulation indicates that this new approach can adapt to different coalescence or breakage kernel function models, and can achieve better prediction for bubble size distribution.

1. Introduction

Bubble columns and their variants including slurry beds and stirred tanks have found widespread applications in chemical and energy-related industries, such as coal liquefaction, waste water treatment and CO_2 utilization, in view of their advantage in mixing, mass and heat transfer. Computational fluid dynamics (CFD) has become an important approach in understanding the complex flow structure of multi-phase flow and the size distribution and interfacial area of bubbles, and therefore in assisting the design, scale-up or optimization of bubble column reactors. However, the CFD simulation for gas-liquid flow is reported to be sensitive to a number of constitutive equations or sub-models. The CFD models currently used for multiphase flow are usually based on the Eulerian-Eulerian framework in which the complex mesoscale physics, e.g., the interaction between the dispersed bubbles and continuous liquid, and the variation of interfacial morphology of dispersed bubbles, is averaged out and hidden in the so-called constitutive equations of two-fluid models, though the governing equations of fluid flow are rigorously derived from continuum mechanics or kinetic theory. The difficulty and challenging issue is therefore shifted to the constitutive models to describe the phase interaction forces (drag, lift and virtual mass forces) for momentum conservation equations and the turbulence models.

Modeling the size distribution of dispersed bubbles is another critical issue. Usually the transport equations for bubble number density, i.e., the population balance equations (PBE), are coupled with CFD equations to calculate the bubble size distribution. The so-called kernel functions for bubble breakup and coalescence is required to model the source terms in PBE, i.e., the birth or death rates of each bubble class. Hitherto most of the kernel functions

* Corresponding author.
E-mail address: nyang@ipe.ac.cn (N. Yang).

http://dx.doi.org/10.1016/j.ces.2017.01.026
0009-2509/

Nomenclature

U_{gas}, U_{liquid} superficial velocities of gas phase and liquid phase, m/s
g gravitational acceleration, m/s^2
M momentum interactions, N/m^3
N_T total energy dissipation, m^2/s^3
N_{surf} dispersed phase surface energy, m^2/s^3
N_{break} breakage energy, m^2/s^3
N_{turb} energy dissipated in turbulence, m^2/s^3
$N_{surf,S}$, $N_{surf,L}$ energy dissipated in turbulence of small bubble phase and large bubble phase, m^2/s^3
$N_{break,S}$, $N_{break,L}$ breakage energy of small bubble phase and large bubble phase, m^2/s^3
C breakage corrector
k turbulence kinetic energy, m^2/s^2
$\tilde{G}_k$ generation of turbulence kinetic energy $\boldsymbol{k}$
G_ω generation of specific dissipation rate $\boldsymbol{\omega}$
Y_k dissipation of $\boldsymbol{k}$ due to turbulence
Y_ω dissipation of $\boldsymbol{\omega}$ due to turbulence
D_ω cross-diffusion term
S_b the source terms of breakage
S_c the source terms of coalescence
d_i droplet diameter, m
f_{BV} the breakage ratio of daughter droplet to its parent droplet
C_1, C_2 and C_3 fitting parameters in Alopaeus model
d_S, d_L diameters of small bubble phase and large bubble phase, m
f_S, f_L volume fractions of small bubble phase and large bubble phase
$U_{g,S}$, $U_{g,L}$ superficial velocities of small bubble phase and large bubble phase, m/s
F_r centripetal force, N
F_D drag force, N
m droplet mass, kg
a the angular acceleration, m/s^2
r radial length along the radial direction, m
C_D drag coefficient
T torque of rotor walls, N m
N rotation speed, rps
$u_{d,\ inlet}$, $u_{C,\ inlet}$ real (interstitial) velocities of dispersed phase and continuous phase at the inlet, m/s
$f_{d,\ inlet}$ volume fraction of dispersed phase at the inlet
l_k Komolgorov length, m
d_{32} Sauter mean diameter, m

Greek letters

ε turbulent kinetic energy dissipation rate, m^2/s^3
ρ_{gas}, ρ_{liquid} densities of gas phase and liquid phase, kg/m^3
Γ mass interactions, kg/(m^3 s^1)

ε_g, ε_s
σ droplet surface tension, N/m
μ dynamic viscosity, Pa s
ω angular velocity, rad/s
λ scale of eddy, m

are based on the combination of isotropic turbulence theory, probability theory and phenomenological models. The CFD-PBM simulation of bubble size distribution is therefore relevant to the turbulence properties, e.g., turbulence dissipation rate, and the model parameters or formulations in kernel functions. There are extensive studies and reviews on population balance modeling of bubble or droplet size distribution (Andersson and Andersson, 2006; Bannari et al., 2008; Bhole et al., 2007; Cheung et al., 2009; Luo and Svendsen, 1996; Wang et al., 2005a,b; Liao and Lucas, 2009, 2010). The Luo and Svendsen model has been successfully used in some recent simulation (Sarhan et al., 2016; Sattar et al., 2013). A recent development is the extension of the fluid particle breakage and coalescence closures to the entire spectrum of isotropic turbulence and a wider range of Reynolds numbers are established based on statistical turbulence theory (Han et al., 2014, 2015; Solsvik and Jakobsen, 2016a, 2016b, 2016c).

Some researchers have coupled the PBM with CFD and the predicted bubble size agreed well with the experiments at low superficial gas velocity (usually $U_g < 0.01$ m/s) or small gas volume fraction (usually $\alpha < 0.1$). But the bubble size was usually over-predicted at relatively higher superficial gas velocity or gas volume fraction, and some empirical correction factors are required to achieve comparable results with experiments. For example, Chen et al. (2004, 2005) found that the breakage rate calculated from the kernel functions of PBM needs to be increased by a factor of ten to match the coalescence rate. Wang et al. (2005a,b) suggested that two effects should be considered to correct the coalescence rate. On one hand, the distance between bubbles may be larger than the bubble turbulent path length and a coefficient less than 1 should be multiplied in the coalescence rate. On the other hand the bubbles occupied a specified volume, and the reduction of free space may increase the coalescence rate. Bhole et al. (2008) held that the over-prediction of coalescence rate was caused by neglecting the slip velocity between the bubble and liquid eddy, a coefficient (<1) related to Stokes number should be used to correct the coalescence kernels. Nguyen et al. (2013) attributed the over-estimation of coalescence rate to the turbulent suppression phenomena. They thought that the liquid turbulent energy of eddy would be converted to the surface energy as the eddy distorted the bubble surface and the eddy size would thus be reduced. This further reduced the contact time and then the coalescence efficiency. Yao and Morel (2004) and Mukin (2014) also pointed out that the corrector was close to 1 for very small gas holdup, and decreased with increasing the gas holdup. Hence the coalescence corrector is not needed at dilute two-phase flow, whereas it turns to be significant in dense flow. Mitre et al. (2010) pointed out that the correctors for breakage and coalescence kernels were necessary to obtain reasonable simulation, and the correctors varied with different breakage and coalescence kernels and superficial velocities. Xu et al. (2013) used the breakage kernel of Luo and Svendsen (1996) and the coalescence model of Luo (1993), and argued that the over-prediction of coalescence rate was caused by the inappropriate turbulence model, and the RNG k-ε model could avoid this problem. Actually a constant coalescence corrector (0.5) was also used in Xu et al. (2013).

Actually each individual element in CFD-PBM simulation of bubble column reactors, e.g., the phase interaction forces (drag, lift and virtual mass forces), turbulence models and kernel functions for bubble breakage and coalescence, is complicated and may interact with each other. In our previous work, we have proposed the Energy-Minimization Multi-Scale (EMMS) approaches for gas-solid (Li and Kwauk, 1994; Yang et al., 2003, 2004), gas-liquid (Yang et al., 2007, 2010; Yang, 2015), gas-liquid-solid (Zhou et al, 2017) and liquid-liquid systems (Qin et al., 2016) respectively. Rather than the reductionism methods which evaluated or investigated each individual element separately in CFD and PBM models,

Please cite this article in press as: Yang, N., Xiao, Q. A mesoscale approach for population balance modeling of bubble size distribution in bubble column reactors. Chem. Eng. Sci. (2017), http://dx.doi.org/10.1016/j.ces.2017.01.026

we proposed that in addition to the averaged mass and momentum conservation equations based on Navier-Stokes equation framework, there should be an additional physical mechanism, i.e., the minimization of meso-scale energy dissipation (stability condition), which drives the evolution of meso-scale structures, e.g., the particle clusters in fast fluidization, or the bubble breakage or coalescence in bubble columns. Based on this concept, we proposed the dual-bubble-size (DBS) model, an extended Energy-Minimization Multi-Scale (EMMS) method for gas-liquid systems. The conceptual model was formulated by some simplified force balance equations and a stability condition considering the compromise of two dominant mechanisms: a liquid-dominant regime at which smaller bubbles prevail and a gas-dominant regime favoring the existence of larger bubbles. Conceptually the model offers a new constraint in addition to the conservative equations of two-fluid model. A new drag law (DBS-drag) was then derived from the DBS model and integrated into the CFD simulation (Yang et al., 2011; Xiao et al., 2013; Xu et al., 2015; Jiang et al., 2015, 2016). The drag model improves the simulation accuracy of the total gas holdup and the radial distribution of gas holdup at various superficial gas velocities. We also noticed that the prediction of flow field and gas holdup was only weakly dependent on the Sauter mean diameter of bubbles which can be specified empirically or obtained from the solution of PBM equations (Yang et al., 2011).

In this paper, we try to extend this method to predict the bubble size distribution. The so-called meso-scale energy dissipation for bubble breakage and coalescence is calculated from the EMMS(DBS) model and then used to provide the correction factors for the coalescence rate in population balance equations. It should be pointed out that here we would not evaluate or investigate each individual element in CFD-PBM simulation, e.g., the turbulence models or kernel functions. These topics have already been extensively reported in literature. In this article we only tentatively propose a new method to provide additional physical mechanisms for a complete description of structure evolution of gas-liquid flow. We first introduce the EMMS(DBS) model for gas-liquid systems, and then the coupling between the EMMS model and population balance equations is established through the meso-scale energy dissipation due to bubble breakage and coalescence. A correction factor for the coalescence rate can therefore be calculated. The CFD-PBM simulation with the correction factor is carried out to model the bubble size distribution in two bubble column reactors, and the simulation is in good agreement with experiments.

2. The CFD-PBM model equations

The mass and momentum conservative equations in two-fluid models are:

$$\frac{\partial(\varepsilon_k\rho_k)}{\partial t}+\nabla\cdot(\varepsilon_k\rho_k\mathbf{u}_k)=\Gamma_k \quad (k=\text{liquid or gas}) \tag{1}$$

$$\frac{\partial(\varepsilon_k\rho_k\mathbf{u}_k)}{\partial t}+\nabla\cdot(\varepsilon_k\rho_k\mathbf{u}_k\mathbf{u}_k)=-\varepsilon_k\nabla P+\mu_{k,eff}\varepsilon_k\left[\nabla\mathbf{u}_k+(\nabla\mathbf{u}_k)^T\right]+\varepsilon_k\rho_k\mathbf{g}+M_{kl} \tag{2}$$

where M_{kl} denotes the momentum interactions between phases, including the drag, lift and virtual mass forces. In this paper, we only consider the drag force as formulated below

$$M_{kl}=\mathbf{F}^D_{gas}=-\mathbf{F}^D_{liquid}=\frac{3}{4}\varepsilon_g\frac{C_D}{d_b}\rho_l|\mathbf{u}_{gas}-\mathbf{u}_{liquid}|(\mathbf{u}_{gas}-\mathbf{u}_{liquid}) \tag{3}$$

Apparently the bubble diameter d_b and the drag coefficient C_D are required to close the model. Generally a Sauter mean bubble diameter was either calculated from PBM or specified empirically (e.g., 4–5 mm), and then used in different drag correlations, such as Schiller-Naumann model, Ishii-Zuber model or Tomiyama model in literature. The Schiller-Naumann model is formulated as

$$C_{D0}=\begin{cases}\frac{24}{Re}(1+0.15Re^{0.687}) & Re\leqslant 1000\\ 0.44 & Re>1000\end{cases} \tag{4}$$

where

$$Re=\frac{\rho u_{slip}d_b}{\mu} \tag{5}$$

It should be pointed out that the bubble diameter is not a prerequisite in the calculation of drag force in Eq. (3) in the two-fluid model since the gas is treated as a continuum and the bubble diameter is only used to calculate the drag force when we simulate the flow field without mass transfer or reactions. Actually we only need the lumped parameter, i.e., the ratio C_D/d_b, to calculate the drag force in Eq. (3), and in our approach the ratio can be derived from the EMMS(DBS) model for air-water systems (Yang et al., 2011; Xiao et al., 2013):

$$(C_D/d_b)_T=\begin{cases}431.14-6729.02U_g+35092.2U_g^2, & U_g\leqslant 0.101\ \text{m/s}\\ 122.49-553.94U_g+741.24U_g^2, & U_g>0.101\ \text{m/s}\end{cases} \tag{6}$$

As the ratio here is only relevant to the overall superficial gas velocity, we termed it as the DBS-Global model. Another version is the so-called DBS-Local model presented in our previous paper (Jiang et al., 2015).

The population balance equation (PBE) for the number density of bubbles is:

$$\frac{\partial}{\partial t}[n(V,x,t)]+\nabla\cdot[\boldsymbol{u}n(V,x,t)]=S \tag{7}$$

where n is the number density as a function of the bubble volume, time and space. S represents the source term for bubble breakup and coalescence and can be formulated as:

$$\begin{aligned}S=&\tfrac{1}{2}\int_0^V c(V-V',V',x,t)n(V-V',x,t)n(V',x,t)dV'\\&-\int_0^\infty c(V,V',x,t)n(V,x,t)n(V',x,t)dV'\\&+\int_{\Omega_V} b(V')\beta(V|V',x,t)n(V',x,t)dV'-b(V,x,t)n(V,x,t)\end{aligned} \tag{8}$$

The four terms at the right hand of Eq. (8) stands for the birth rate of bubbles of volume V due to the coalescence of two smaller bubbles, the death rate of bubbles of volume V due to their coalescence with other bubbles, the birth rate of bubbles of volume V due to the breakage of larger bubbles and the death rate of bubbles of volume V due to their breakage respectively. Here c and b denote the coalescence and breakage rates, and β represents the daughter particle size distribution function, all of which are required to model through the so-called kernel functions. β can be defined as:

$$\beta(f_v,d)=\frac{2b(f_v,d)}{\int_0^1 b(f_v,d)df_v} \tag{9}$$

where f_v denotes the breakage fraction ($v_{daughter}/v$). There have been a number of theoretical or empirical breakage and coalescence models proposed in literature (Liao and Lucas, 2009, 2010). Among them, the breakage kernels of Luo and Svendsen (1996) and Lehr et al. (2002) and the coalescence models of Luo (1993) and Prince and Blanch (1990) are most commonly used in CFD-PBM simulation. It should be noticed that in the original model of Prince and Blanch (1990), the collisional frequency in the coalescence kernel

Please cite this article in press as: Yang, N., Xiao, Q. A mesoscale approach for population balance modeling of bubble size distribution in bubble column reactors. Chem. Eng. Sci. (2017), http://dx.doi.org/10.1016/j.ces.2017.01.026

Table 1
Breakage and coalescence kernels.

Breakage kernels	
Luo and Svendsen (1996)	$b(f_v,d)=0.923(1-\alpha_g)\left(\frac{\varepsilon}{d^3}\right)^{1/3}\int_{\xi_{\min}}^{1}\frac{(1+\xi)^2}{\xi^{11/3}}\exp\left(-\frac{12c_f\sigma}{\beta\rho_l\varepsilon^{2/3}d^{5/3}\xi^{11/3}}\right)d\xi$ $b(d)=\int_0^{0.5}b(f_v,d)df_v$ $f_v=\frac{v_{daughter}}{v}$ $c_f=f_v^{2/3}+(1-f_v)^{2/3}-1$ $\xi=\frac{\lambda}{d}$ λ is the arriving eddy size
Lehr et al. (2002)	$b(f_v,d)=\int_{d'}^{d}1.19\frac{\sigma}{\rho_f\varepsilon^{2/3}d'^4}\frac{(\lambda+d)^2}{\lambda^{13/3}}\exp\left(-\frac{2\sigma}{\rho_f\varepsilon^{2/3}d'}\frac{1}{\lambda^{2/3}}\right)d\lambda$ $b(d)=\int_0^{0.5}b(f_v,d)df_v$ d' is the diameter of smaller daughter bubble
Coalescence kernels $c(d_i,d_j)=\varpi_c P_c$ $P_c=\exp(-t_{ij}/\tau_{ij})$ t_{ij} is the coalescence time and τ_{ij} is the contact time	
Prince and Blanch (1990)	$\varpi_c(d_i,d_j)=0.089\pi\varepsilon^{1/3}(d_i+d_j)^2(d_i^{2/3}+d_j^{2/3})^{1/2}$ $P_c(d_i,d_j)=\exp\left(-\frac{r_{ij}^{5/6}\rho_l^{1/2}\varepsilon^{1/3}}{4\sigma^{1/2}}\ln\frac{h_0}{h_f}\right)$ $r_{ij}=\frac{1}{4}\frac{d_id_j}{d_i+d_j}$ h_0 and h_f are the initial and final film thickness and 10^{-4} and 10^{-8} for air-water system respectively
Luo (1993)	$\varpi_c(d_i,d_j)=\frac{\pi}{4}\sqrt{2}\varepsilon^{1/3}(d_i+d_j)^2(d_i^{2/3}+d_j^{2/3})^{1/2}$ $P_c(d_i,d_j)=\exp\left(-0.4\frac{[0.75(1+\xi_{ij}^2)(1+\xi_{ij}^3)]^{1/2}}{\left(\frac{\rho_g}{\rho_l}+0.5\right)^{1/2}(1+\xi_{ij})^3}We_{ij}^{1/2}\right)$ $We_{ij}=\frac{\rho_l d_i\bar{u}_{ij}^2}{\sigma}$ $\bar{u}_{ij}=(\bar{u}_i^2+\bar{u}_j^2)^{1/2}=\bar{u}_i\left(1+\xi_{ij}^{-2/3}\right)$, $\xi_{ij}=\frac{d_i}{d_j}$, $\bar{u}_i=\sqrt{2\varepsilon d_i}$

includes three parts, i.e., the collision due to turbulence, buoyancy-driven or laminar shear. In this paper, only the turbulence collision is considered for bubble columns. All the breakage and coalescence kernels used in this paper are listed in Table 1. It should be pointed out that some kernel functions are reported not to be conservative in volume or number (Solsvik et al., 2013) and the appropriate energy spectrum model was not considered (Solsvik and Jakobsen, 2016a, 2016b). However our approach essentially does not rely on specific kernel functions, and the stability condition provides another physical constraint to calculate the coalescence rate.

When the number density function (n) is obtained from the population balance equation, the Sauter mean bubble diameter can be calculated and fed into the drag models in TFM such as Schiller-Naumann model (Schiller and Naumann, 1935), Ishii-Zuber model (Ishii and Zuber, 1979) or Tomiyama model (Tomiyama, 1998):

$$d_{32}=\frac{\sum_i n_i d_i^3}{\sum_i n_i d_i^2} \tag{10}$$

It should be pointed out that this Sauter diameter is not required in the DBS drag model as mentioned earlier. Only the lumped parameter, i.e., the ratio of drag coefficient to bubble diameter is needed and can be calculated directly from the DBS model.

3. The EMMS model for gas-liquid systems

In the EMMS(DBS) model for gas-liquid systems (Yang et al., 2007, 2010), the flow structure of the system was resolved into small bubbles, large bubbles and liquid phase, and can be described by six structure variables (d_i, α_i and $U_{g,i}$) representing the diameter, volume fraction and superficial velocity of small and larger bubbles respectively. We can then formulate three simplified force and mass balance equations for the six variables:

$$U_{g,S}+U_{g,L}=U_g \tag{11}$$

$$f_S(\rho_l-\rho_g)g=\frac{f_s}{\pi/6d_S^3}C_{D,S}\frac{\pi}{4}d_S^2\frac{1}{2}\rho_l\left(\frac{U_{g,S}}{f_S}-\frac{U_l}{1-f_b}\right)^2 \tag{12}$$

$$f_L(\rho_l-\rho_g)g=\frac{f_L}{\pi/6d_L^3}C_{D,L}\frac{\pi}{4}d_L^2\frac{1}{2}\rho_l\left(\frac{U_{g,L}}{f_L}-\frac{U_l}{1-f_b}\right)^2 \tag{13}$$

A stability condition is proposed to close the model equations, i.e., the minimization of microscale energy dissipation or maximization of mesoscale energy dissipation. The energy dissipation terms are expressed as functions of structure parameters and the six structure parameters can be obtained by solving the nonlinear optimization problem. The total energy dissipation N_T was grouped into three portions, i.e., N_{surf}, N_{turb} and N_{break}. We noticed that only a part of the total energy N_T is directly transferred from bubbles to liquids through the process of energy cascade of liquid turbulence (N_{turb}). The remaining part is either consumed in the bubble surface oscillation or deformation (N_{surf}), or deposited temporarily as the surface energy generated through bubble breakage and is then released to the liquid bulk phase through bubble coalescence and finally dissipated (N_{break}). The former two portions are directly dissipated at micro-scale and the latter is stimulated, transferred or stored temporarily at "mesoscale". Actually the latter serves as a buffer for energy dissipation in gas-liquid systems and is used to sustain the formation and evolution of mesoscale structure. All these three parts of energy are contributed to bubble breakage and coalescence processes, whereas only the effect of N_{turb} (turbulent energy dissipation) was considered in the previous CFD-PBM simulations in literature.

Please cite this article in press as: Yang, N., Xiao, Q. A mesoscale approach for population balance modeling of bubble size distribution in bubble column reactors. Chem. Eng. Sci. (2017), http://dx.doi.org/10.1016/j.ces.2017.01.026

When larger bubbles are broken into smaller daughter bubbles, the energy dissipated in surface oscillation and deformation N_{surf} decreases and this process is governed by some extremum tendency, i.e., $N_{surf} \rightarrow$ min. When smaller bubbles coalesce into larger bubbles, the energy dissipation through liquid turbulence N_{turb} decreases, and $N_{turb} \rightarrow$ min to favor the formation of large bubbles. In practice, breakup and coalescence may reach a dynamic equilibrium at steady state, which can mathematically described by a stability condition $N_{surf} + N_{turb} \rightarrow$ min. It can also be understood as the minimization of microscale energy dissipation or conveyed as the maximization of mesoscale energy dissipation $N_{break} \rightarrow$ max since the total energy N_T fed into the system is invariable at steady state. The stability condition can physically supply the closure laws for the drag force in the momentum conservation equations of two-fluid models or kernel functions of breakage or coalescence in the population balance equations, i.e., the conservation equations for bubble number density. The different energy dissipation terms is formulated as the functions of structure parameters, as listed below:

$$N_{surf} = \left(1 - \frac{C_{D,p}}{C_{D,b}}\right) N_T \tag{14}$$

$$N_{break} = \int_{\lambda_{\min}}^{d_b} \int_0^{0.5} \frac{\varpi(d_b, \lambda)}{(1-f_b)\rho_l + f_b \rho_g} P_b(d_b, \lambda, f_{BV}) c_f \pi d_b^2 \sigma df_{BV} d\lambda \tag{15}$$

$$N_{turb} = N_T - N_{surf} - N_{turb} = U_g g - N_{surf} - N_{turb} \tag{16}$$

The calculation of structure parameters and different energy terms has been reported in our previous publications. For brevity we only introduce the general concept and model framework of the EMMS(DBS) model since this article focuses on its integration with CFD and PBM models. More details about the physical background and model analysis can be referred to Yang et al. (2007, 2010, 2011), Yang (2015) and Chen et al. (2009). It should be pointed out that the model is a zero-dimensional conceptual model, and the energy dissipation terms are calculated from the so-called average structure parameters which roughly reflect the evolution system structure. The model includes several simplified force and mass balance equations and a stability condition, and the only input parameter is the overall superficial gas velocity. It is therefore not comparable with the turbulence properties obtained from CFD simulation or the isotropic turbulence theory. The conceptual structure parameters and energy terms are used to qualitatively understand the evolution of the system, and we could further derive some closure models for drag force or coalescence models.

4. Integration with CFD-PBM model equations

We are now in a position to integrate the EMMS(DBS) model with CFD-PBM model framework by deriving a corrector through a simplified PBE in which the transient terms are neglected and only the source terms are kept, as illustrated in Fig. 1. Firstly with the specified information of the global flow field (U_g, U_l) and physical properties of gas and liquid, the six structure parameters and the different energy dissipation terms (N_{turb}, N_{surf}, $N_{break\text{-}DBS}$) can be obtained simultaneously. Then an iteration process is implemented between the simplified PBE and the DBS model. Given a trial value of the coalescence corrector C, the simplified population balance equation can be solved to acquire the bubble number density n_i for each bubble class, and then the energy stored at meso-scale, $N_{break\text{-}PBM}$, can be calculated from an equation similar to Eq. (15). By comparing the meso-scale energy dissipation term given by the DBS model ($N_{break\text{-}DBS}$) with the term $N_{break\text{-}PBM}$ given by the simplified PBE, we can determine the corrector C_{DBS} which can finally equalize the two terms by some iterative calculation. As the DBS model takes the meso-scale energy dissipation (N_{break}) into consideration, C_{DBS} essentially reflects of the constraint of meso-scale energy dissipation due to bubble breakage and coalescence. In this way the stability condition, i.e., the minimization of micro-scale energy dissipation or the maximization of the meso-

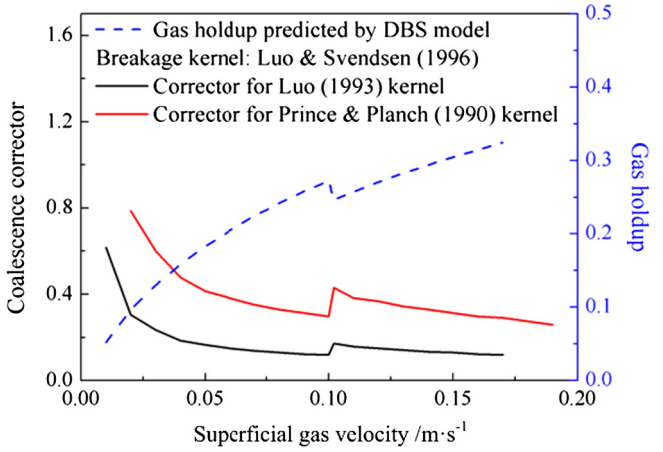

Fig. 2. Correction factors for different coalescence kernels (Breakage kernel: Luo & Svendsen).

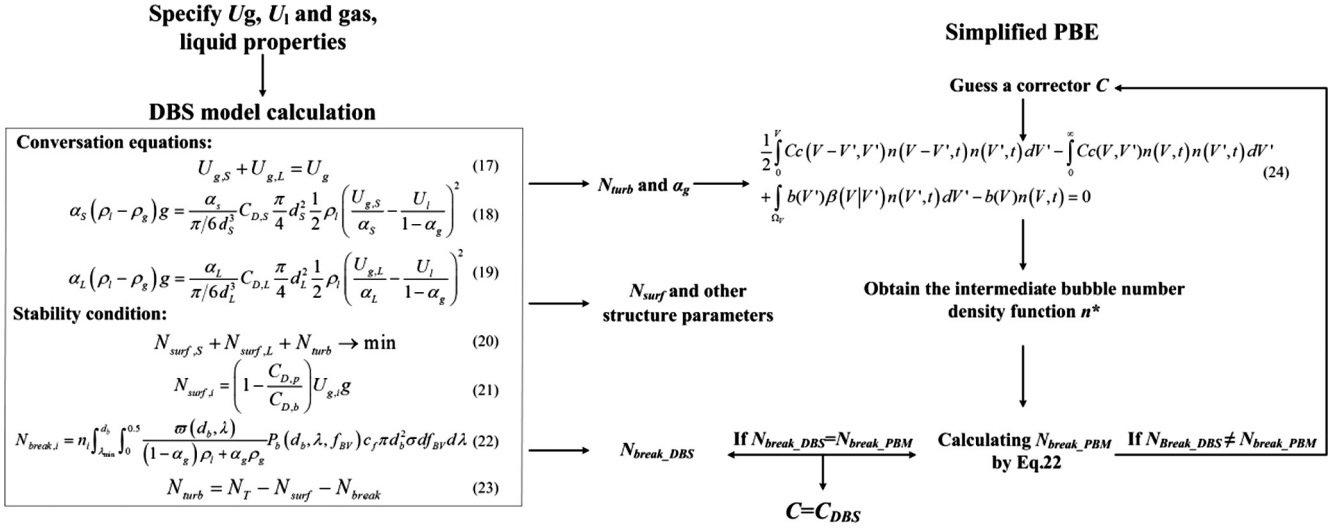

Fig. 1. Flow chart of obtaining correction factor C_{DBS}.

scale energy dissipation, is incorporated into the calculation of the correctors for kernel functions, and serves as another physical constraint for bubble number density in addition to the PBM conservation equations. The correction factor C_{DBS} can then be used in the CFD-PBM model equations. It should also be noticed that the correction factor C_{DBS} for coalescence rate actually reflects the joints effects of breakage and coalescence. This is because only the source terms of birth and death rates due to breakage and coalescence is kept in the simplified PBE, as shown in the right part of Fig. 1. Hence the correction factor is only multiplied in the source terms of coalescence kernels.

Ideally, the coalescence corrector should be updated for each cell at each time step in CFD-PBM simulation if we could feed the model with the information of local flow field into the DBS model. However this process may be computationally time-consuming. Here we only use the information for the whole system at the given conditions (U_g, U_l and gas and liquid properties), and hence the correction factor obtained is now only a function of superficial gas velocity and physical properties. Although further work could be carried out to refine the model, we can demonstrate that this approximation is reasonable through the CFD-PBM simulation in the following sections.

Fig. 2 shows the calculation results of C_{DBS} for air-water systems. C_{DBS} decreases with superficial gas velocity and the decrease gradually slows down. It should be noticed that different breakage or coalescence kernels lead to different C_{DBS}. The curve-fitted formulas for C_{DBS} are:

$$C_{DBS} = \begin{cases} 0.29733 + 1.25303\exp^{-\frac{Ug}{0.02119}} & Ug \leqslant 0.101\ \text{m/s} \\ 0.21454 + 1.04371\exp^{-\frac{Ug}{0.06278}} & Ug > 0.101\ \text{m/s} \end{cases} \quad (17)$$

for the breakage kernel of Luo and Svendsen (1996) and the coalescence kernel of Prince and Blanch (1990),

$$C_{DBS} = \begin{cases} 0.13491 + 1.13403\exp^{-\frac{Ug}{0.01148}} & Ug \leqslant 0.101\ \text{m/s} \\ 0.10164 + 0.53737\exp^{-\frac{Ug}{0.04961}} & Ug > 0.101\ \text{m/s} \end{cases} \quad (18)$$

for the breakage kernel of Luo and Svendsen (1996) and the coalescence kernel of Luo (1993).

At low superficial gas velocity, the dispersed phase (bubbles) is dilute and usually spherical, homogeneously distributed in the continuous phase. Bubble coalescence is not so strong as that at high flow rates. The traditional CFD-PBM method may still work and the coalescence correctors should be close to 1, which can be reflected by the trend of the curve in Fig. 2. The corrector decreases with increasing the superficial gas velocity. It should be noticed that there is a jump change on the curve which corresponds to the regime transition between the homogeneous and fully-developed heterogeneous regimes. More details about the jump change have been discussed in our previous work (Yang et al., 2007, 2010; Chen et al., 2009).

5. Bubble columns and numerical configuration

The bubble columns of Bhole et al. (2006) and McClure et al. (2013) were simulated in this paper. The information of those two columns is summarized in Table 2 and Fig. 3. The original column height was 1 m in the experiments of Bhole et al. (2006). In our simulation the column height was augmented to 1.8 m to avoid the liquid escape from the top, and this treatment does not change the aspect ratio (H/D). The sparger was modeled as a velocity inlet and the boundary condition at the top was set as the pressure outlet. Other boundaries were set as no-slip wall conditions. Dispersed RNG k-ε turbulence model was applied as recommended by Laborde-Boutet et al. (2009). First order up-wind method was used to discretize the momentum equations. The flow was simulated for 160 s of physical time and the data was averaged over the last 80 s.

The PBE was solved by the method of class. As suggested by Bhole et al. (2008), it is reasonable to discretize the continuous bubble size distribution into 13 discrete classes ranging from 1 mm to 25 mm, and set the inlet bubble size as 5 mm. For the McClure system, since the superficial gas velocity was higher and larger bubbles may appear, the bubbles was divided into 20 classes ranging from 1 mm to 39 mm and the inlet bubble size was set as 5 mm. The simulations were implemented by Ansys Fluent, and the closure models like drag coefficient and the new breakup and coalescence kernels were incorporated through the user defined functions (UDF).

The CFD-PBM simulation using the new corrector is then validated with the two cases of experiments, i.e., the Bhole case operated at $U_g = 0.02$ m/s and the McClure case operated at $U_g = 0.04$ m/s or $U_g = 0.11$ m/s. The DBS correctors using in the simulation can be calculated from Eqs. (17), (18) and are also presented in Table 3.

For comparison, we also used the correction factor proposed by Bhole et al. (2008) which is a function of Stokes number:

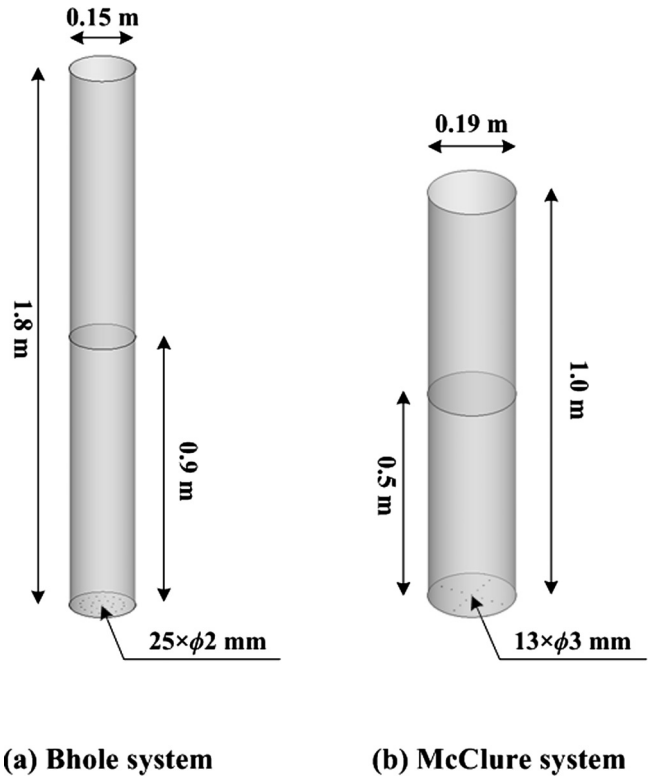

Fig. 3. Schematic view of simulated bubble columns.

Table 2
Bubble columns simulated.

Bubble columns	Column diameter (m)	Column height (m)	Static liquid height (m)	Spargers (mm)	Superficial gas velocity (m/s)	Mesh
Bhole et al. (2006)	0.15	1.8	0.9	25 × 2	Air-water: 0.02	441,445
McClure et al. (2013)	0.19	1	0.5	13 × 3	Air-water: 0.04 Air-fermentation: 0.04, 0.11	397,895

Please cite this article in press as: Yang, N., Xiao, Q. A mesoscale approach for population balance modeling of bubble size distribution in bubble column reactors. Chem. Eng. Sci. (2017), http://dx.doi.org/10.1016/j.ces.2017.01.026

Table 3
DBS correction factors for coalescence rate.

	Working liquid	Superficial gas velocity (m/s)	Correction corrector for coalescence kernels	
			Luo model	Prince & Blanch model
Bhole case	Air-water	0.02	0.3054	0.7873
McClure case	Air-water	0.04		0.4764
	Air-fermentation	0.04		0.4585
		0.11		0.1840

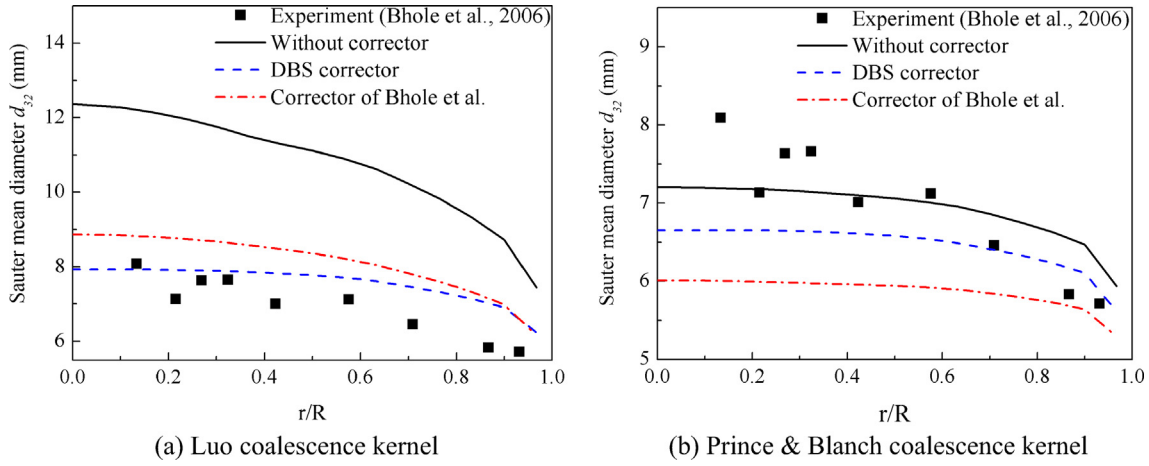

Fig. 4. Sauter bubble diameter predicted by C_{DBS} (z = 0.6 m, drag model: Schiller-Naumann, breakage kernel: Luo & Svendsen).

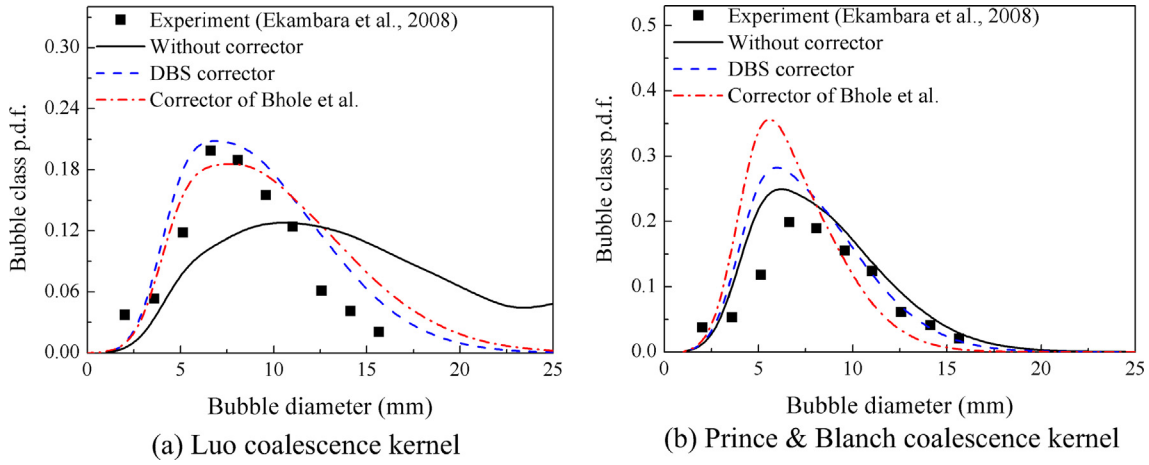

Fig. 5. Gas holdup-based probability distribution of bubble classes predicted by C_{DBS} (z = 0.9 m, drag model: Schiller-Naumann, breakage kernel: Luo & Svendsen).

$$C_{Bhole} = \sqrt{\frac{1}{1+St}} \tag{19}$$

$$St = \frac{\tau_B}{\tau_f} \tag{20}$$

$$\tau_B = \frac{4C_V d_B}{3C_D V_B} \tag{21}$$

$$\tau_f = C_\mu^{3/4}\frac{k}{\varepsilon} \tag{22}$$

$$C_V = 0.5(1+4\alpha)(0.37Re\cdot \mathrm{Mo}^{0.23}+1) \tag{23}$$

6. Results and discussion

6.1. Bhole case

The original Luo & Svendsen breakage kernel was first adopted for the simulation of Bhole case, and we then applied the new corrector models. Figs. 4 and 5 present the Sauter mean bubble diameter and bubble size distribution predicted by the CFD-PBM simulation respectively. Here the Schiller-Naumann drag model is used in Figs. 4 and 5. The bubble size varies significantly when using different coalescence kernels and correctors. C_{DBS} for Luo coalescence kernel is 0.3054 (Table 3), which means that the coalescence rate would be reduced by >2/3. Thus the predicted bubble size with C_{DBS} was much smaller than that by the original coalescence kernel and agrees well with the experimental data (Figs. 4 and 5a). Both C_{Bhole} and C_{DBS} greatly improved the bubble size predictions compared to the original Luo coalescence kernel. Compared to the prediction of C_{Bhole}, the CFD-PBM simulation with C_{DBS} has better performances in both the prediction of Sauter mean diameter and bubble size distribution. For the Luo coalescence model (Fig. 5a), the Bhole corrector model predicts much more larger bubbles than the experiment data, and the DBS corrector model improves the simulation of larger bubbles.

Please cite this article in press as: Yang, N., Xiao, Q. A mesoscale approach for population balance modeling of bubble size distribution in bubble column reactors. Chem. Eng. Sci. (2017), http://dx.doi.org/10.1016/j.ces.2017.01.026

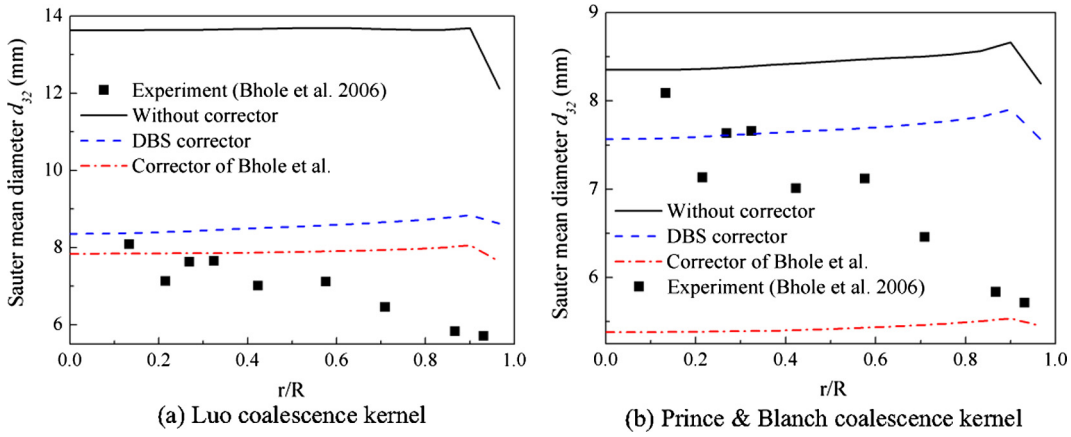

Fig. 6. Sauter bubble diameter using C_{DBS} (z = 0.6 m, drag model: DBS, breakage kernel: Luo & Svendsen).

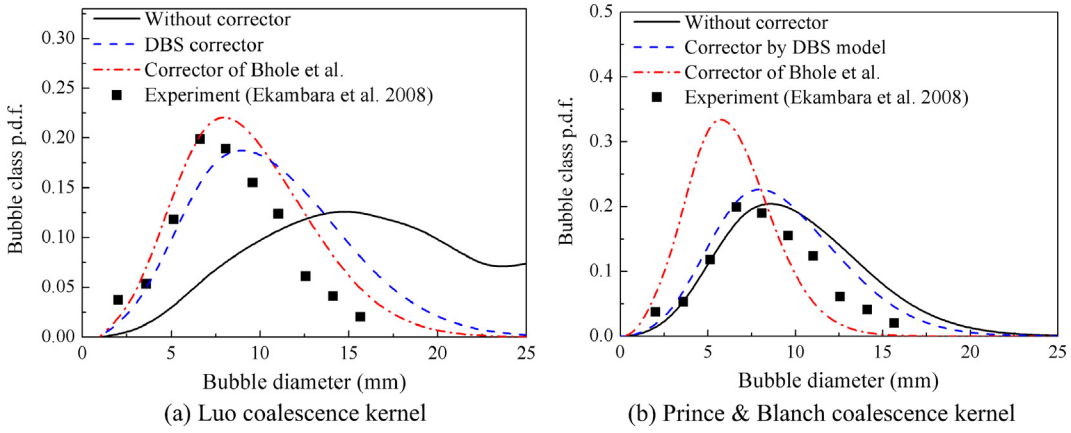

Fig. 7. Gas holdup-based probability distribution of bubble classes using the DBS corrector C_{DBS} (z = 0.9 m, drag model: DBS, breakage kernel: Luo & Svendsen).

For the Prince & Blanch coalescence kernel, the DBS corrector C_{DBS} is close to 1(0.7873), which indicates that no significant correction is needed in this situation. As the CFD-PBM simulation using the Luo & Svendsen (breakage) and Prince & Blanch (coalescence) kernels offers satisfied bubble size prediction, the value of C_{DBS} is reasonable. It can be observed from Fig. 4b that the CFD-PBM simulation with C_{DBS} slightly under-estimates the Sauter mean diameter at the center but performs well at the wall region. The Bhole corrector predicts much smaller Sauter mean diameter and correspondingly a peak of smaller bubbles in bubble size distribution, as shown in Fig. 5b. Hence for the Prince & Blanch coalescence (Fig. 5b), the Bhole corrector model predicts much smaller bubbles and less larger bubbles than the experimental data. In contrast, the DBS corrector model largely improves the prediction. In particular, the large bubble population is correctly predicted.

Compared to the Bhole corrector C_{Bhole} which only works well for the specific breakage and coalescence kernels, the DBS corrector has acceptable accuracy in bubble size prediction for different combinations of coalescence and breakage kernels. This means the corrector derived from the DBS model could self-adapt the kernel functions used, implying that the stability condition plays a critical role in calculating the coalescence or breakage rate.

Actually the drag model has little influence on the bubble size distribution though it could improve the prediction of gas holdup as demonstrated in our previous studies (Yang et al., 2011; Xiao et al., 2013). The DBS drag model is used in Figs. 6 and 7. When using the DBS drag model, the original Luo coalescence kernel also greatly over-predicted the bubble size whereas the Prince & Blanch kernel performs better. The radial distribution of Sauter mean diameter predicted by the DBS drag model is slightly different from that by Schiller-Naumann drag model (Figs. 4 and 5). For the coalescence kernel of Luo (1993), the CFD-PBM simulations with both

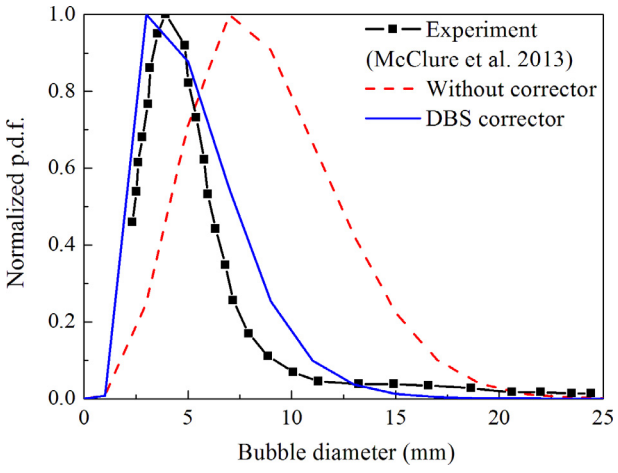

Fig. 8. Gas holdup-based probability distribution of bubble classes (air-water system, U_g = 4 cm/s, breakage kernel: Luo & Svendsen, coalescence kernel: Prince & Blanch).

Please cite this article in press as: Yang, N., Xiao, Q. A mesoscale approach for population balance modeling of bubble size distribution in bubble column reactors. Chem. Eng. Sci. (2017), http://dx.doi.org/10.1016/j.ces.2017.01.026

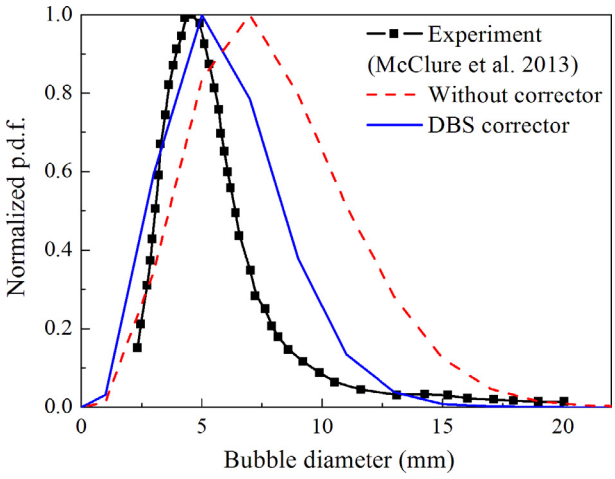

Fig. 9. Gas holdup-based probability distribution of bubble classes (air-fermentation system, U_g = 4 cm/s, breakage kernel: Luo & Svendsen, coalescence kernel: Prince & Blanch).

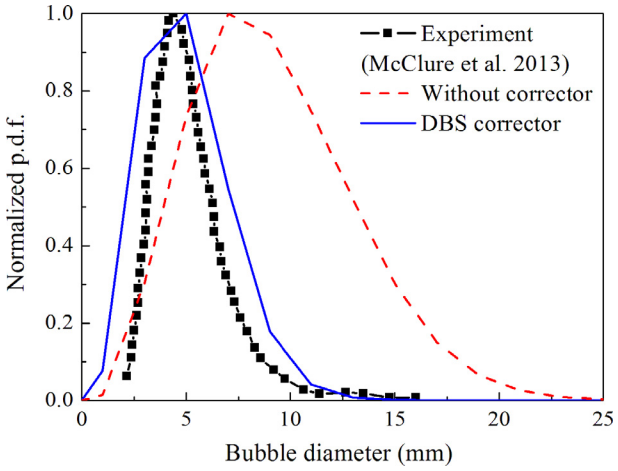

Fig. 10. Gas holdup-based probability distribution of bubble classes (air-fermentation system, U_g = 11 cm/s, breakage kernel: Luo & Svendsen, coalescence kernel: Prince & Blanch).

the C_{Bhole} and C_{DBS} could reasonably predict the bubble size at the column center and slightly over-predict that at the wall region (Fig. 6). For the coalescence kernel of Prince and Blanch (1990), the original kernel slightly over-predicted the bubble size and the corrector C_{Bhole} obviously under-estimated the bubble diameter. By contrast both the d_{32} and bubble size distribution agreed well with the experimental data using the C_{DBS}. In this case, the corrector of DBS model C_{DBS} works well for different breakage and coalescence kernels and different drag models, whereas other previous correctors (C_{Bhole} and C_{chen}) are only applicable for specified breakage or coalescence kernels.

6.2. McClure case

The McClure case (for both air-water and air-fermentation systems) is simulated to further validate the DBS corrector model C_{DBS} at higher superficial gas velocities for both the air-water and air-fermentation systems. Only the Luo and Svendsen (1996) breakage and Prince and Blanch (1990) coalescence kernels are used herein. The viscosity of fermentation liquid is 0.002 Pa s and the surface tension is about 0.03571 N/m. The detailed column information is summarized in Table 2 and Fig. 1.

Fig. 8 compares the BSD predicted by CFD-PBM with experimental measurements at the superficial gas velocity 4 cm/s. The equilibrium size is usually located in the range of 4–6 mm for the air-water systems, as reported in the literatures (McClure et al., 2013; Polli et al., 2002; Camarasa et al., 1999). Although the combination of Luo & Svendsen breakage and Prince & Blanch coalescence kernels works well at the superficial gas velocity 2 cm/s as mentioned earlier, these kernels significantly over-predict the bubble diameter at U_g = 4 cm/s (d_{32} = 7.32 mm), which means that the corrector is necessary to obtain the reasonable BSD at different superficial gas velocities. When using the DBS corrector C_{DBS} (0.4764), the simulation results agree well with the experimental data (d_{32} = 4.46 mm), which further validates the DBS corrector model.

We also simulated the air-fermentation system and Figs. 9 and 10 compare the normalized bubble size distribution predicted by CFD-PBM simulations with experimental data. Without using the corrector, the CFD-PBM significantly over-estimates the bubble size at both the superficial gas velocities. When using the DBS corrector C_{DBS}, the BSD predictions have been greatly improved, which means that the coalescence corrector is necessary not only for the air-water system, but also for the air-fermentation system. For both the air-water and air-fermentation systems, the DBS corrector C_{DBS} can generate reasonable bubble size distribution.

The above simulations show the advantage of this approach and the new corrector model in this paper. It can improve the prediction of bubble size distribution compared to the original kernel models and the corrector models in literature. The new corrector model can also adapt and be suitable for different kernel function models. It should be pointed out that the focus of the new approach is not just in the new corrector model. It essentially provides another constraint to coalescence or breakage rates, i.e., using N_{break} to close the PBE. Theoretically it can be used to calculate the whole coalescence or breakage rate. However to integrate the new approach into current model framework of kernel functions and utilize the information of the local value of turbulence dissipate rate in CFD, we applied a prefactor (corrector) in front of the kernel functions in literature. This simple treatment does not affect its physical significance.

In future, more validation of this new approach and the new corrector model should be carried out for different bubble column systems operated under various flow rates. Moreover, the correctors in this paper are now only a function of the overall superficial gas velocity, so that the correctors for each local cell of CFD simulation are the same. This limitation could be eliminated by further applying the approach to each cell. Furthermore, more kernel functions, in particular, the recent study on the development new kernel functions which relate the turbulence properties and the coalescence or breakage rates with consideration of the new energy spectrum model could be integrated with this approach.

7. Conclusion

Current Kernel functions for bubble coalescence and breakage is based on statistical or phenomenological models with empirical parameters, and the CFD-PBM simulation with these kernel functions usually over-estimates the bubble size with increasing the superficial gas velocity or gas holdup, even using the RNG k-ε model for turbulence or considering the capillary constraint in breakage kernels as recommended in literature. We propose a new approach based on the Energy-minimization multiscale concept. The so-called mesoscale energy dissipation and the stability condition serves as another physical constraint for bubble number density in addition to the kernel functions which relates the turbulence dissipation rate to the coalescence or breakage rates. A new

Please cite this article in press as: Yang, N., Xiao, Q. A mesoscale approach for population balance modeling of bubble size distribution in bubble column reactors. Chem. Eng. Sci. (2017), http://dx.doi.org/10.1016/j.ces.2017.01.026

corrector model for coalescence rate is then derived. Our CFD-PBE simulation with the new corrector indicates that the new corrector can improve the prediction of the Sauter mean bubble size and the bubble size distribution compared to the original kernel models for coalescence and the corrector models in literature. New model can also adapt the kernel functions for coalescence used and give different correctors.

Acknowledgements

The authors wish to acknowledge the long term support from the National Natural Science Foundation of China (Grant Nos 91434121, 91634203), the Chinese Academy of Sciences (Grant No. 122111KYSB20150003).

References

Andersson, R., Andersson, B., 2006. Modeling the breakup of fluid particles in turbulenct flows. AIChE J. 52, 2031–2038.
Bhole, M.R., Joshi, J.B., Ramkrishna, D., 2007. Population balance modeling for bubble columns operating in the homogeneous regime. AIChE J. 53, 579–588.
Bhole, M.R., Joshi, J.B., Ramkrishna, D., 2008. CFD simulation of bubble columns incorporating population balance modeling. Chem. Eng. Sci. 63, 2267–2282.
Bannari, R., Kerdouss, F., Selma, B., Bannari, A., Proulx, P., 2008. Three-dimensional mathematical modeling of dispersed two-phase flow using class method of population balance in bubble columns. Comput. Chem. Eng. 32, 3224–3237.
Bhole, M.R., Roy, S., Joshi, J.B., 2006. Laser doppler anemometer measurements in bubble column: effect of sparger. Ind. Eng. Chem. Res. 45, 9201–9207.
Chen, P., Sanyal, J., Dudukovic, M.P., 2004. CFD modeling of bubble columns flows: implementation of population balance. Chem. Eng. Sci. 59, 5201–5207.
Chen, P., Sanyal, J., Dudukovic, M.P., 2005. Numerical simulation of bubble columns flows: effect of different breakup and coalescence closures. Chem. Eng. Sci. 60, 1085–1101.
Chen, J., Yang, N., Ge, W., Li, J., 2009. Modeling of regime transition in bubble columns with stability condition. Ind. Eng. Chem. Res. 48, 290–301.
Cheung, S.C.P., Yeoh, G.H., Tu, J., 2009. A review of population balance modelling for isothermal bubbly flows. J. Computat. Multiphase Flow. 1, 161–199.
Camarasa, E., Vial, C., Poncin, S., Wild, G., Midoux, N., Bouillard, J., 1999. Influence of coalescence behaviour of the liquid and of gas sparging on hydrodynamics and bubble characteristics in a bubble column. Chem. Eng. Process. 38, 329–344.
Han, L., Gong, S., Li, Y., Gao, N., Fu, J., Luo, H., Liu, Z., 2014. Influence of energy spectrum distribution on drop breakage in turbulent flows. Chem. Eng. Sci. 117, 55–70.
Han, L., Gong, S., Ding, Y., Fu, J., Gao, N., Luo, H., 2015. Consideration of low viscous droplet breakage in the framework of the wide energy spectrum and the multiple fragments. AIChE J. 61, 2147–2168.
Ishii, M., Zuber, N., 1979. Drag coefficient and relative velocity in bubbly, droplet or particulate flows. AIChE Journal 25, 843–855.
Jiang, X., Yang, N., Yang, B., 2016. Computational fluid dynamics simulation of hydrodynamics in the riser of an external loop airlift reactor. Particuology 27, 95–101.
Jiang, X., Yang, N., Zhu, J., Yang, B., 2015. On the single and two-bubble class models for bubble column reactors. Chem. Eng. Sci. 123, 514–526.
Li, J., Kwauk, M., 1994. Particle-Fluid Two-Phase Flow—The Energy-Minimization Multi-Scale Method. Metallurgical Industry Press, Beijing. 204.
Luo, H., Svendsen, H., 1996. Theoretical model for drop and bubble breakup in turbulent dispersions. AIChE J. 42, 1225–1233.
Luo, H., 1993. Coalescence, Breakup and Liquid Circulation in Bubble Column Reactors: Department of Energy. Norges Tekniske Hoegskole, Trondheim.
Liao, Y., Lucas, D., 2010. A literature review on mechanisms and models for the coalescence process of fluid particles. Chem. Eng. Sci. 65, 2851–2864.
Liao, Y., Lucas, D., 2009. A literature review of theoretical models for drop and bubble breakup in turbulent dispersions. Chem. Eng. Sci. 64, 3389–3406.
Lehr, F., Millies, M., Mewes, D., 2002. Bubble-size distributions and flow fields in bubble columns. AIChE J. 48, 2426–2443.
Laborde-Boutet, C., Larachi, F., Dromard, N., Delsart, O., Schweich, D., 2009. CFD simulation of bubble column flows: investigations on turbulence models in RANS approach. Chem. Eng. Sci. 64, 4399–4413.
Mukin, R.V., 2014. Modeling of bubble coalescence and break-up in turbulent bubbly flow. Int. J Multiphas. Flow 62, 52–66.
Mitre, J.F., Takahashi, R.S.M., Ribeiro Jr, C.P., Lage, P.L.C., 2010. Analysis of breakage and coalescence models for bubble columns. Chem. Eng. Sci. 65, 6089–6100.
McClure, D.D., Kavanagh, J.M., Fletcher, D.F., Barton, G.W., 2013. Development of a CFD model of bubble column bioreactors: part one – a detailed experimental study. Chem. Eng. Technol. 36, 2065–2070.
Nguyen, V.T., Song, C.-H., Bae, B.-U., Euh, D.-J., 2013. Modeling of bubble coalescence and break-up considering turbulent suppression phenomena in bubbly two-phase flow. Int. J. Multiphas. Flow 54, 31–42.
Prince, M.J., Blanch, H.W., 1990. Bubble coalescence and break-up in air-sparged bubble-columns. AIChE J. 36, 1485–1499.
Polli, M., Stanislao, M.D., Bagatin, R., Bakr, E.A., Masi, M., 2002. Bubble size distribution in the sparger region of bubble columns. Chem. Eng. Sci. 57, 197–205.
Qin, C., Chen, C., Xiao, Q., Yang, N., Yuan, C., Kunkelmann, C., 2016. Cetinkaya M., Mülheims K., CFD-PBM simulation of droplets size distribution in rotor-stator mixing devices. Chem. Eng. Sci. 155, 16–26.
Schiller, L., Naumann, A., 1935. A drag coefficient correlation. Vdi Zeitung 77, 318–320.
Sarhan, A.R., Naser, J., Brooks, G., 2016. CFD simulation on influence of suspended solid particles on bubbles' coalescence rate in flotation cell. Int. J. Mineral Process 146, 54–64.
Sattar, M.A., Naser, J., Brooks, G., 2013. Numerical simulation of two-phase flow with bubble break-up and coalescence coupled with population balance modeling 70, 66–76.
Solsvik, J., Jakobsen, H.A., 2016a. Development of fluid particle breakup and coalescence closure models for the complete energy spectrum of isotropic turbulence. Ind. Eng. Chem. Res. 55, 1449–1460.
Solsvik, J., Jakobsen, H.A., 2016b. A review of the statistical turbulence theory required extending the population balance closure models to the entire spectrum of turbulence. AIChE J. 62, 1795–1820.
Solsvik, J., Tangen, S., Jakobsen, H.A., 2013. On the constitutive equations for fluid particle breakage. Rev. Chem. Eng. 29 (5), 241–356.
Tomiyama, A., 1998. Struggle with computational bubble dynamics. Multiphase Sci. Tech. 10, 369–405.
Solsvik, J., Skjervold, V.T., Han, L., Luo, H., Jakobsen, H.A., 2016. A theoretical study on drop breakup modeling in turbulent flows: The inertial subrange versus the entire spectrum of isotropic turbulence. Chem. Eng. Sci. 149, 249–265.
Wang, T., Wang, J., Jin, Y., 2005a. Population balance model for gas-liquid flows: influence of bubble coalescence and breakup models. Ind. Eng. Chem. Res. 44, 7540–7549.
Wang, T., Wang, J., Jin, Y., 2005b. Theoretical prediction of flow regime transition in bubble columns by the population balance model. Chem. Eng. Sci. 60, 6199–6209.
Xiao, Q., Yang, N., Li, J., 2013. Stability-constrained multi-fluid CFD models for gas–liquid flow in bubble columns. Chem. Eng. Sci. 100, 279–292.
Xu, L.J., Yuan, B.R., Ni, H.Y., Chen, C.X., 2013. Numerical simulation of bubble column flows in churn-turbulent regime: comparison of bubble size models. Ind. Eng. Chem. Res. 52, 6794–6802.
Xu, T., Jiang, X., Yang, N., Zhu, J., 2015. CFD simulation of internal-loop airlift reactor using EMMS drag model. Part 19, 124–132.
Yang, N., Wu, Z., Chen, J., Wang, Y., Li, J., 2011. Multi-scale analysis of gas–liquid interaction and CFD simulation of gas–liquid flow in bubble columns. Chem. Eng. Sci. 66, 3212–3222.
Yang, N., Chen, J., Ge, W., Li, J., 2010. A conceptual model for analyzing the stability condition and regime transition in bubble columns. Chem. Eng. Sci. 65, 517–526.
Yao, W., Morel, C., 2004. Volumetric interfacial area prediction in upward bubbly two-phase flow. Int. J. Heat. Mass. Tran. 47, 307–328.
Yang, N., Chen, J., Zhao, H., 2007. Explorations on the multi-scale flow structure and stability condition in bubble columns. Chem. Eng. Sci. 62, 6978–6991.
Yang, N., 2015. Mesoscale transport phenomena and mechanisms in gas-liquid reaction systems. In: Marin, G.B., Li, J. (Eds.), Advance in Chemical Engineering, vol. 46. Burlington.
Yang, N., Wang, W., Ge, W., Li, J., 2003. CFD simulation of concurrent-upgas-solid flow incirculating fluidized beds with structure-dependent drag coefficient. Chem. Eng. Sci. 96, 71–80.
Yang, N., Wang, W., Ge, W., Li, J., 2004. Simulationofheterogeneousstructureina circulating fluidized-bed riserbycombiningthetwo-fluid model with the EMMS approach. Ind. Eng. Chem. Res. 43, 5548–5561.
Zhou, R., Yang, N., Li, J., 2017. CFD simulation of gas-liquid-solid flow in slurry bubble columns with EMMS drag model. Powder Tech. 10. http://dx.doi.org/10.1016/j.powtec.2016.09.083.

Please cite this article in press as: Yang, N., Xiao, Q. A mesoscale approach for population balance modeling of bubble size distribution in bubble column reactors. Chem. Eng. Sci. (2017), http://dx.doi.org/10.1016/j.ces.2017.01.026